Available online at www.sciencedirect.com
SCIENCE DIRECT
ELSEVIER
Journal of the European Ceramic Society 26 (2006) 2069–2074
ECERS
www.elsevier.com/locate/jeurceramsoc

Microwave dielectric properties of $BaO–Ta_2O_5–TiO_2$ system

Atsushi Yokoi *, Hirotaka Ogawa, Akinori Kan

Faculty of Science and Technology, Meijo University, 1-501 Shiogamaguchi, Tempaku-ku, Nagoya 468-8502, Japan

Available online 14 November 2005

Abstract

Microwave dielectric properties of the $BaO–Ta_2O_5–TiO_2$ system were investigated by the solid-state reaction method. It was recognized that the $Ba_{10}Ta_{7.04}(Ti_{1.2-x}Sn_x)O_{30}$ solid solutions have the higher $Q \cdot f$ value in comparison with the $Ba_8(Ta_{4-x}Nb_x)Ti_3O_{24}$ solid solutions. The limit of the $Ba_{10}Ta_{7.04}(Ti_{1.2-x}Sn_x)O_{30}$ solid solutions was approximately $x = 0.75$; the lattice parameter c of the solid solutions, which is related to the change in the $B(1)O_6$ octahedron, was significantly increased in the composition range from 0 to 0.75. The $Q \cdot f$ values of the $Ba_{10}Ta_{7.04}(Ti_{1.2-x}Sn_x)O_{30}$ solid solutions are remarkably improved by the Sn substitution for Ti; the highest $Q \cdot f$ value of 59,100 GHz is obtained at $x = 0.75$. Moreover, the ε_r and τ_f values of the $Ba_{10}Ta_{7.04}(Ti_{1.2-x}Sn_x)O_{30}$ solid solutions at $x = 0.75$ were 25.6 and 30.3 ppm/°C, respectively.

Keywords: Powders-solid state reaction; Dielectric properties; TiO_2; Perovskites

1. Introduction

Most of the commercially used microwave dielectric ceramics have a perovskite-type crystal structure; a variety of microwave dielectric ceramics with such perovskite-type structure have been studied to date.[1–3] The $Ba(Mg_{1/3}Ta_{2/3})O_3$ (BMT) compound is one and it has a 1:2 cation ordering of *B*-site; this material is well known to have a high quality factor ($Q \cdot f$) of 350,000 GHz, a dielectric constant (ε_r) of 25 and a temperature coefficient of resonant frequency (τ_f) of 2 ppm/°C.[4] Thus, the complex oxides with a perovskite-type structure are considered to be attractive candidates for use in a wireless communication technology which requires a combination of a relatively high dielectric constant, a high $Q \cdot f$ value and a near zero temperature coefficient of resonant frequency. The continuous development of wireless communication technology will rely upon the identification of new dielectric ceramics with the appropriate microwave dielectric properties as described above.

In recent work that focused on the crystal structure analysis of perovskite-like structures, Shpanchenko et al.[5] reported the crystal structures of $Ba_8Ta_4Ti_3O_{24}$ and $Ba_{10}Ta_{7.04}Ti_{1.2}O_{30}$ compounds; these compounds have the complex perovskite-like structures with space group of $P6_3/mcm$ and $P6_3/mmc$, respectively. However, the microwave dielectric properties of $Ba_8Ta_4Ti_3O_{24}$ and $Ba_{10}Ta_{7.04}Ti_{1.2}O_{30}$ compounds have not been clarified to date. Thus, the $Ba_8(Ta_{4-x}Nb_x)Ti_3O_{24}$ and $Ba_{10}Ta_{7.04}(Ti_{1.2-x}Sn_x)O_{30}$ solid solutions were prepared by solid state reaction method; the microwave dielectric properties-crystal structure relationship of the solid solutions were investigated in this study.

2. Experimental method

High-purity (>99.9%) $BaCO_3$, Ta_2O_5, Nb_2O_5, TiO_2 and SnO_2 powders weighed on the basis of their stoichiometric composition were mixed and calcined at 1100 °C for 10 h in air. These calcined powders were milled and mixed with a polyvinyl alcohol, and then pressed into a pellet of 12 mm in diameter and 7 mm in thickness under the pressure of 100 MPa. Subsequently, these pellets of $Ba_8(Ta_{4-x}Nb_x)Ti_3O_{24}$ and $Ba_{10}Ta_{7.04}(Ti_{1.2-x}Sn_x)O_{30}$ solid solutions were sintered at the various temperatures ranging from 1430 °C to 1450 °C and from 1530 °C to 1650 °C for 10 h in air, respectively. The crystalline phases were identified by the X-ray powder diffraction (XRPD). The lattice parameters and crystal structures of the samples were refined by using the Rietveld analysis (RIETAN).[6,7] Moreover, the morphological changes in the samples were investigated by using a field emission scanning electron microscopy (FE-SEM) and energy dispersive X-ray (EDX) spectroscopy. The dielectric constants and the quality factors were measured by the Hakki–Coleman method.[8] The τ_f values were determined from the difference between the resonant frequencies obtained at 20 °C and 80 °C.

* Corresponding author.

0955-2219/$ – see front matter © 2005 Elsevier Ltd. All rights reserved.
doi:10.1016/j.jeurceramsoc.2005.09.061

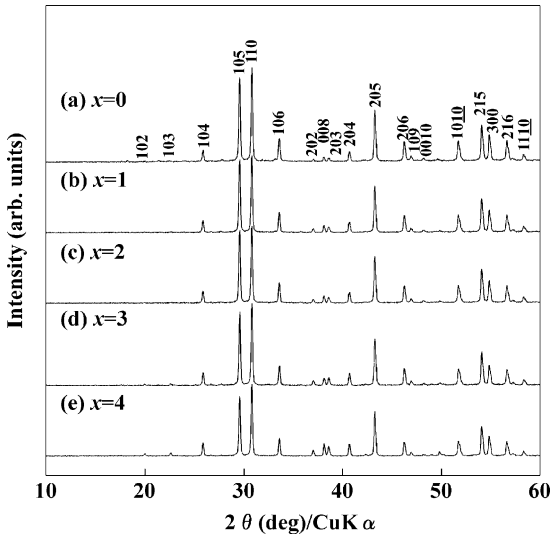

Fig. 1. XRPD patterns of $Ba_8(Ta_{4-x}Nb_x)Ti_3O_{24}$ ($x = 0$, 1, 2, 3 and 4) solid solutions.

3. Results and discussion

3.1. $Ba_8(Ta_{4-x}Nb_x)Ti_3O_{24}$ solid solutions

XRPD patterns of $Ba_8(Ta_{4-x}Nb_x)Ti_3O_{24}$ solid solutions are shown in Fig. 1. From the XRPD results of Nb-substituted $Ba_8(Ta_{4-x}Nb_x)Ti_3O_{24}$ solid solutions, no secondary phase was detected over the whole composition range. The solid solutions are identified to be a hexagonal crystal structure with $P6_3/mcm$ space group as reported by Shpanchenko et al.[5] The lattice parameters and the unit cell volumes of $Ba_8(Ta_{4-x}Nb_x)Ti_3O_{24}$ solid solutions are shown in Fig. 2 and the detail on these values are listed in Table 1. The lattice parameter a was increased slightly with increasing composition x, whereas the lattice parameter c varied linearly. Thus, as the lattice parameters varied linearly throughout the entire composition range, the $Ba_8(Ta_{4-x}Nb_x)Ti_3O_{24}$ solid solutions satisfy Vegard's Law, which confirms the formation of solid solutions. The unit cell volumes of $Ba_8(Ta_{4-x}Nb_x)Ti_3O_{24}$ solid solutions were slightly decreased by the Nb substitution for Ta; the decrease in the unit cell volume of the solid solution depended upon the variations in the lattice parameter c.

The microwave dielectric properties of $Ba_8(Ta_{4-x}Nb_x)Ti_3O_{24}$ solid solutions are shown in Fig. 3. The ε_r values of the solid solutions range from 34.1 to 38.1 and the variations of those have not been remarkable in the solid solutions ($x = 0$–4). The $Q \cdot f$ values of the solid solutions decreased from 23,000 to 12,700 GHz, depending on the composition x. The highest $Q \cdot f$ value of 23,000 GHz was obtained at $x = 0$, and so the Nb substitution for Ta is not effective in improving the $Q \cdot f$ values in this system. The temperature coefficients of resonant frequency range from 75.8 to 124.9 ppm/°C; therefore, the substitution of the other elements in this system is necessary in order to improve the τ_f values.

Table 1
Lattice parameters and unit cell volumes of $Ba_8(Ta_{4-x}Nb_x)Ti_3O_{24}$ solid solutions

Composition x	Lattice parameter (Å)		Unit cell volume (Å^3)
	a	c	
0	10.0334(2)	18.8670(4)	1644.88(7)
1	10.0340(2)	18.8621(5)	1644.64(8)
2	10.0342(1)	18.8571(6)	1644.28(1)
3	10.0334(5)	18.8544(7)	1643.77(1)
4	10.0341(2)	18.8530(4)	1643.56(3)

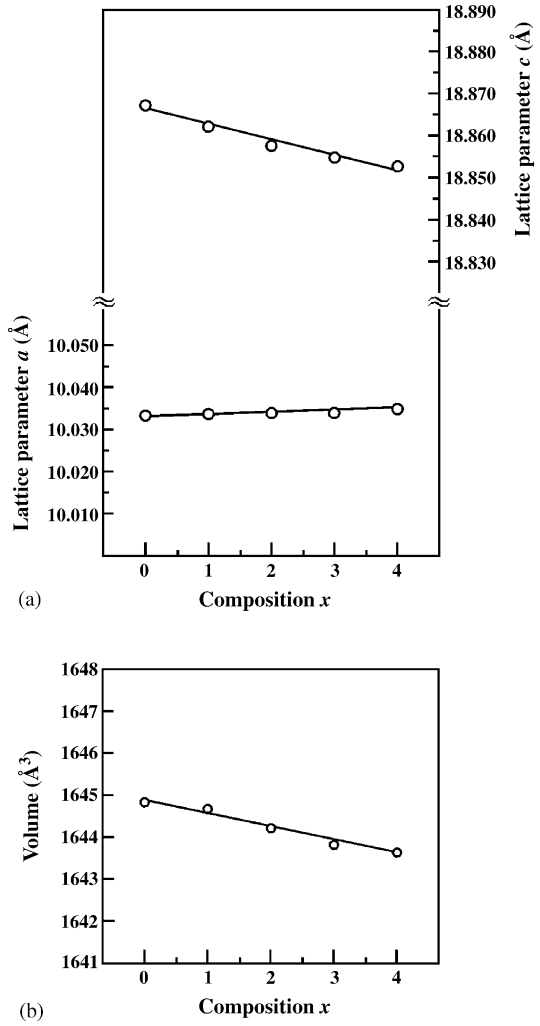

Fig. 2. Effects of Nb substitution for Ta on lattice parameters and unit cell volumes of $Ba_8(Ta_{4-x}Nb_x)Ti_3O_{24}$ ($x = 0$, 1, 2, 3 and 4) solid solutions as a function of composition x.

The microstructures of the $Ba_8(Ta_{4-x}Nb_x)Ti_3O_{24}$ solid solutions were investigated by using the FE-SEM in order to clarify the effects of Nb substitution for Ta on the microwave dielectric properties. The FE-SEM photographs of $Ba_8(Ta_{4-x}Nb_x)Ti_3O_{24}$ solid solutions sintered at 1430 °C for 10 h in air are shown in Fig. 4. Although the grain sizes of $Ba_8(Ta_{4-x}Nb_x)Ti_3O_{24}$ solid solutions were increased with increasing composition x, the formation of porosities and secondary phases was not observed in the compositions ranging from 0 to 4. It is generally known that the variations in the $Q \cdot f$ values are closely related to the morphological changes in the microwave dielectric ceramics.[9]

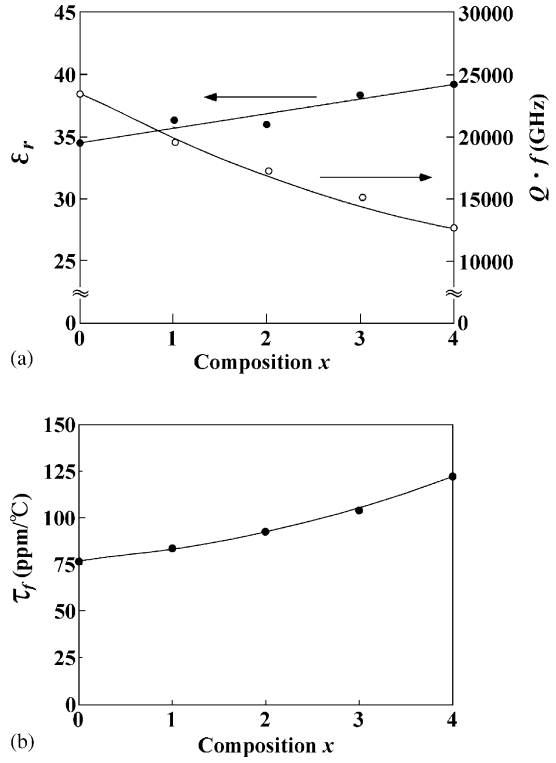

Fig. 3. Microwave dielectric properties of $Ba_8(Ta_{4-x}Nb_x)Ti_3O_{24}$ ($x = 0$, 1, 2, 3 and 4) solid solutions as a function of composition x.

The increase of the grain size reduces the dielectric loss, though the increase of the grain size in $Ba_8(Ta_{4-x}Nb_x)Ti_3O_{24}$ solid solutions increased the dielectric loss. However, the result of Al_2O_3 was showed at the single composition. In this study, the morphological changes in the samples, which arise from the compositional changes in the solid solutions, are observed as shown in Fig. 4. Thus, it is considered that the compositional change in the samples may exert an influence on the variations in $Q \cdot f$ value, because the composition x of each solid solutions were not of same composition.

3.2. $Ba_{10}Ta_{7.04}(Ti_{1.2-x}Sn_x)O_{30}$ solid solutions

Fig. 5 shows the XRPD patterns of $Ba_{10}Ta_{7.04}(Ti_{1.2-x}Sn_x)O_{30}$ solid solutions sintered at 1580 °C for 10 h in air. The XRPD results showed the presence of four phases ($Ba_5Ta_4O_{15}$, $Ba_4Ta_2O_9$, SnO_2 and an unknown phase) at $x = 1.2$ instead of the formation of $Ba_{10}Ta_{7.04}Sn_{1.2}O_{30}$ compound, whereas the samples in the compositions ranged from 0 to 0.75 showed a single

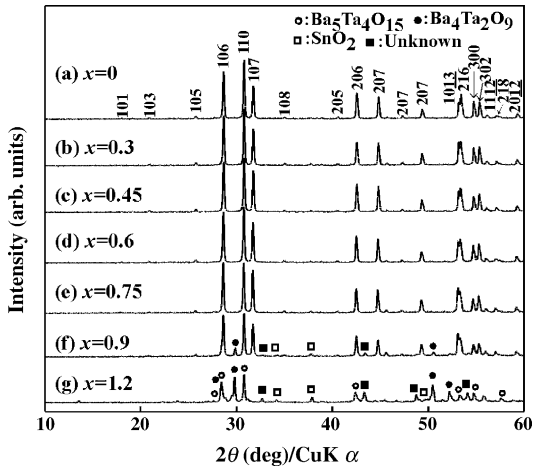

Fig. 5. XRPD patterns of $Ba_{10}Ta_{7.04}(Ti_{1.2-x}Sn_x)O_{30}$ ($x = 0$, 0.3, 0.45, 0.6, 0.75, 0.9 and 1.2) solid solutions.

Table 2
Lattice parameters and unit cell volumes of $Ba_{10}Ta_{7.04}(Ti_{1.2-x}Sn_x)O_{30}$ solid solutions

Composition x	Lattice parameter (Å)		Unit cell volume (Å^3)
	a	c	
0	5.8022(5)	23.7951(1)	693.76(1)
0.3	5.8078(1)	23.8208(5)	695.86(3)
0.45	5.8098(1)	23.8312(5)	696.63(3)
0.6	5.8112(1)	23.8430(5)	697.31(3)
0.75	5.8139(2)	23.8571(6)	698.38(4)
0.9	5.8155(4)	23.8742(8)	699.25(6)
1.2	5.8164(5)	23.8617(8)	699.11(6)

phase, which was a hexagonal crystal structure with $P6_3/mmc$ space group. In the crystal structure of $Ba_{10}Ta_{7.04}Ti_{1.2}O_{30}$ ceramic, two types of the corner-sharing octahedra, i.e., $B(1)O_6$, $B(2)O_6$ and $B(3)O_6$, are present in the unit cell; these octahedra are occupied by the Ta and Ti atoms. The site occupancies of Ta and Ti cations in the B-site of $B(1)O_6$ and $B(2)O_6$ octahedra are known to be 0.9 and 0.1, respectively, whereas the site occupancies of Ta and Ti ions and oxygen vacancy in the B-site in $B(3)O_6$ octahedron is 0.41, 0.15 and 0.44, respectively.[5] In order to clarify the influence of the difference in ionic radii between Ti^{4+} and Sn^{4+} ions on the crystal structure, the lattice parameters of the solid solutions were determined by the Rietveld method, and the results obtained are shown in Fig. 6 and Table 2. The lattice parameters, a and c, of $Ba_{10}Ta_{7.04}(Ti_{1.2-x}Sn_x)O_{30}$ solid solutions ($x = 0$–0.75) are increased linearly with increasing the

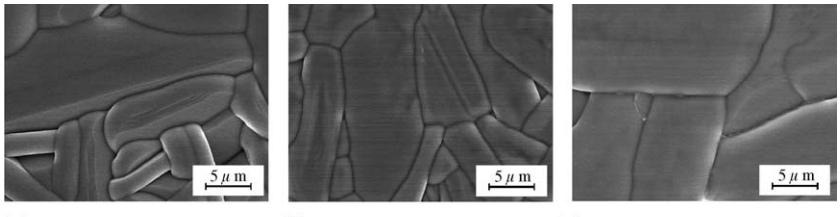

Fig. 4. FE-SEM photographs of $Ba_8(Ta_{4-x}Nb_x)Ti_3O_{24}$ ($x = 0$, 2 and 4) solid solutions sintered at 1430 °C for 10 h in air.

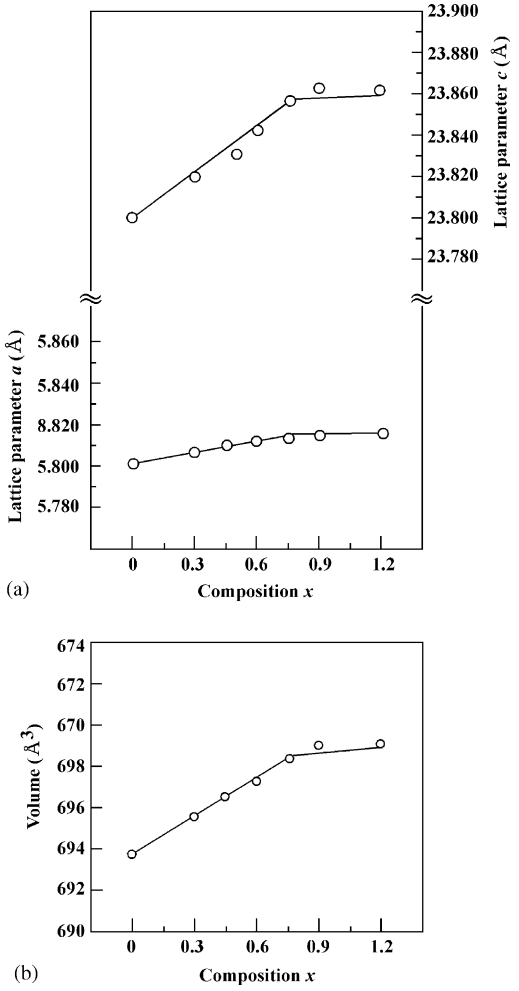

Fig. 6. Effects of Sn substitution for Ti on lattice parameters of $Ba_{10}Ta_{7.04}(Ti_{1.2-x}Sn_x)O_{30}$ solid solutions as a function of composition x.

Table 3
Atomic distances of $B(1)O_6$, $B(2)O_6$ and $B(3)O_6$ polyhedron

Atomic distances (Å)	$Ba_{10}Ta_{7.04}(Ti_{1.2-x}Sn_x)O_{24}$ solid solutions	
	$x=0$: $B1$ = Ti	$x=0.75$: $B1$ = Sn
$B(1)$–O(2)	1.998	2.003
O(2)–O(2)	2.832	2.908
O(2)–O′(2)	2.82	2.76
O′(2)–O′(2)	2.832	2.908
O(2)–O″(2)	2.82	2.76
O′(2)–O″(2)	2.82	2.76
	$Ba_{10}Ta_{7.04}(Ti_{1.2-x}Sn_x)O_{24}$ solid solutions	
	$x=0$: $B2$ = Ti	$x=0.75$: $B2$ = Sn
$B(2)$–O′(2)	2.10	2.11
$B(2)$–O′(3)	2.379	2.267
O(2)–O(2)	2.99	3.06
O(2)–O′(2)	2.94	2.92
O(2)–O(3)	2.94	2.92
O(2)–O′(3)	3.76	3.46
O(3)–O(3)	3.76	3.46
O(3)–O′(3)	2.94	2.92
	$Ba_{10}Ta_{7.04}(Ti_{1.2-x}Sn_x)O_{24}$ solid solutions	
	$x=0$: $B3$ = Ti	$x=0.75$: $B3$ = Ti
$B(3)$–O′(1)	2.075	2.085
$B(3)$–O′(3)	1.916	1.95
O(1)–O(1)	2.04	3.04
O(1)–O′(1)	2.04	3.04
O(1)–O(3)	3.044	2.98
O(1)–O′(3)	3.044	2.98
O(3)–O(3)	3.04	2.35
O(3)–O′(3)	3.04	2.35

composition x, and then these lattice parameters are approximately constant in the composition range of 0.9–1.2. Therefore, it is recognized that the limit of the solid solutions is approximately $x=0.75$.

The variations in the atomic distances of $B(1)O_6$, $B(2)O_6$ and $B(3)O_6$ octahedra caused by the Sn substitution for Ti were shown in Fig. 7 and Table 3. In the $B(1)O_6$ polyhedron, the increases in oxygen-oxygen distances such as O(2)–O(2) and O′(2)–O′(2) were observed with the Sn substitution for Ti. Since the direction of the O(2)–O(2) and O′(2)–O′(2) distances in the $B(1)O_6$ polyhedron is parallel to that of the c-axis, it is considered that the increase in the lattice parameter c as shown in Fig. 6 closely relates with the variations in the atomic distances of O(2)–O(2) and O′(2)–O′(2). Moreover, these variations of the lattice parameters and the atomic distances were related to the changes in the volume of each octahedron. The effects of Sn substitution for Ti on the volume of polyhedron in $Ba_{10}Ta_{7.04}(Ti_{1.2-x}Sn_x)O_{30}$ solid solutions in the single phase region are shown as a function of composition x in Fig. 8. The volumes of the $B(1)O_6$, $B(2)O_6$ and $B(3)O_6$ octahedra were constant with all the samples in the composition range from 0 to 0.75, whereas a linear dependence of volume in the $Ba(1)O_{12}$, $Ba(2)O_{12}$ and $Ba(3)O_{12}$ polyhedra on the composition x was observed; the volume of the $Ba(2)O_{12}$ and $Ba(3)O_{12}$ polyhedra slightly increased. Furthermore, the volume of the $Ba(1)O_{12}$ polyhedra significantly decreased with increasing the composition x.

The microwave dielectric properties of $Ba_{10}Ta_{7.04}(Ti_{1.2-x}Sn_x)O_{30}$ solid solutions are shown in Fig. 9. With increased composition x from 0 to 0.75, the ε_r values of the solid solutions varied from 35.0 to 26.5; at the compositions higher than $x=0.75$, the ε_r values were drastically decreased because of the presence of a secondary phase. The $Q\cdot f$ values of $Ba_{10}Ta_{7.04}(Ti_{1.2-x}Sn_x)O_{30}$ solid solutions at the composition range from 0 to 0.75 vary from 33,200 to 59,100 GHz, and the maximum $Q\cdot f$ value is obtained at $x=0.75$. The Sn substitution for Ti is effective in improving the $Q\cdot f$ values in this system. Moreover, the τ_f values of the solid solutions in the composition range of 0–0.75 vary from 52.0 to 30.3 ppm/°C; a near zero τ_f values was not obtained, though the $Q\cdot f$ value of the solid solutions was improved by Sn substitution for Ti.

In order to clarify the relationship between the microstructure and the $Q\cdot f$ values caused by Sn substitution for Ti, the microstructural changes in $Ba_{10}Ta_{7.04}(Ti_{1.2-x}Sn_x)O_{30}$ solid solutions were investigated by using the FE-SEM and EDX. Fig. 10 shows the FE-SEM photographs of $Ba_{10}Ta_{7.04}(Ti_{1.2-x}Sn_x)O_{30}$ solid solution at $x=0$, 0.6 and 1.2,

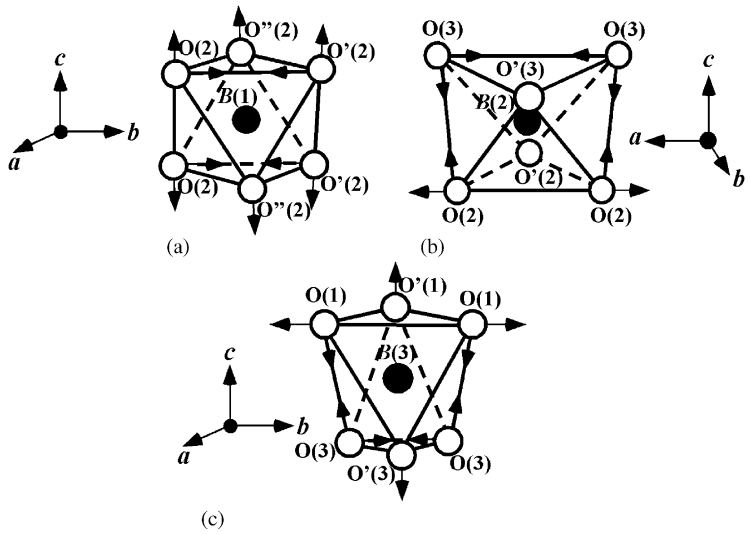

Fig. 7. Variations in atomic distances of $B(1)O_6$, $B(2)O_6$ and $B(3)O_6$ octahedra in $Ba_{10}Ta_{7.04}(Ti_{1.2-x}Sn_x)O_{30}$ ($x = 0$ to 0.75) solid solutions caused by Sn substitution for Ti.

respectively. When comparing these microstructures, porosity is not observed at $x = 0$ and 0.6, whereas a number of porosities and cracks are recognized at $x = 1.2$; it is known that the formation of porosity and cracks lowers the ε_r and $Q \cdot f$ values of the solid solutions.[9] The EDX results of the samples marked *A*, *B* and *C* were found to be $Ba_5Ta_4O_{15}$, $Ba_4Ta_2O_9$ and an unknown phase,

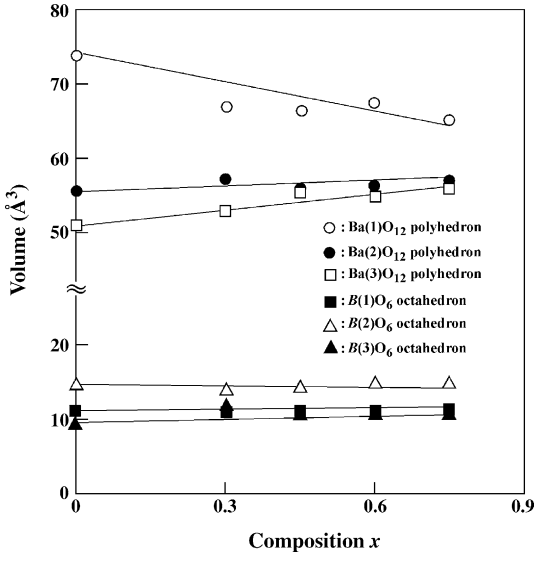

Fig. 8. Variations in volume of $Ba(1)O_{12}$, $Ba(2)O_{12}$, $Ba(3)O_{12}$ polyhedra and $B(1)O_6$, $B(2)O_6$ and $B(3)O_6$ octahedra as a function of composition x.

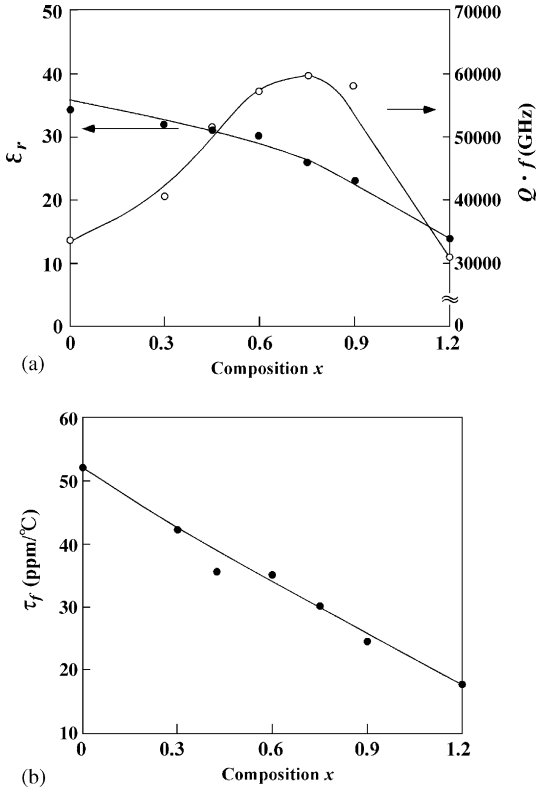

Fig. 9. Variations in dielectric constants (ε_r) and quality factors ($Q \cdot f$) of $Ba_{10}Ta_{7.04}(Ti_{1.2-x}Sn_x)O_{30}$ solid solutions as a function of composition x.

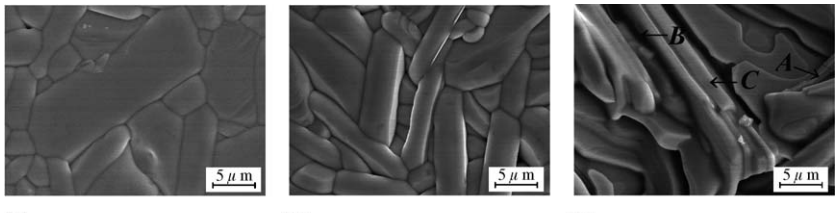

Fig. 10. FE-SEM photographs of $Ba_{10}Ta_{7.04}(Ti_{1.2-x}Sn_x)O_{30}$ ($x = 0$, 0.6 and 1.2) solid solutions.

respectively. From these results, it is considered that the formation of secondary phase exerts an influence on the decrease in ε_r and $Q \cdot f$ values at the compositions higher than $x = 0.75$.

4. Conclusions

The hexagonal perovskite-like solid solutions, i.e., $Ba_8(Ta_{4-x}Nb_x)Ti_3O_{24}$ and $Ba_{10}Ta_{7.04}(Ti_{1.2-x}Sn_x)O_{30}$ solid solutions, were synthesized; the microwave dielectric properties of the solid solutions were investigated. When comparing the microwave dielectric properties of $Ba_8(Ta_{4-x}Nb_x)Ti_3O_{24}$ solid solutions with those of $Ba_{10}Ta_{7.04}(Ti_{1.2-x}Sn_x)O_{30}$ solid solutions, a high $Q \cdot f$ value was obtained in the $Ba_{10}Ta_{7.04}(Ti_{1.2-x}Sn_x)O_{30}$ solid solutions. In the $Ba_{10}Ta_{7.04}(Ti_{1.2-x}Sn_x)O_{30}$ solid solutions, the limit of solid solutions was approximately $x = 0.75$.

It was found that the variations in the lattice parameters closely related to the variations in the atomic distances of $Ba_{10}Ta_{7.04}(Ti_{1.2-x}Sn_x)O_{30}$ solid solutions, which arises from the differences in the ionic radii of Sn^{4+} and Ti^{4+} ions. In particular, the increase in the lattice parameter c was responsible for the variations in the atomic distances of the $B(1)O_6$ octahedron.

As for the microwave dielectric properties of $Ba_{10}Ta_{7.04}(Ti_{1.2-x}Sn_x)O_{30}$ solid solutions, the Sn substitution for Ti was effective in improving the $Q \cdot f$ value; a dielectric constant of 25.6, a $Q \cdot f$ value of 59,100 GHz and a τ_f value of 30.3 ppm/°C were obtained at $x = 0.75$.

References

1. Davies, P. K., Borisevich, A. and Thirumal, M., Communicating with wireless perovskites: cation order and zinc volatilization. *J. Eur. Ceram. Soc.*, 2003, **23**, 2461–2466.
2. Desu, S. B. and O'Bryan, H. M., Microwave loss quality of $BaZn_{1/3}Ta_{2/3}O_3$ ceramics. *J. Am. Ceram. Soc.*, 1985, **68**, 546–551.
3. Vineis, C., Davies, P. K., Negas, T. and Bell, S., Microwave dielectric properties of hexagonal perovskites. *Mater. Res. Bull.*, 1996, **31**, 431–437.
4. Tamura, H., Konoike, T., Sakabe, Y. and Wakino, K., Improved high Q dielectric resonator with complex perovskite structure. *J. Am. Ceram. Soc.*, 1984, **67**, C59–C61.
5. Shpanchenko, P. V., Nistor, L., Van Tendeloo, G., Van Landuyt, J. and Amelinckx, S., Structure studies on new ternary oxides $Ba_8Ta_4Ti_3O_{24}$ and $Ba_{10}Ta_{7.04}Ti_{1.2}O_{30}$. *J. Solid State Chem.*, 1995, **114**, 560–574.
6. Rietveld, H. M., Profile refinement method for nuclear and metal urinates. *J. Appl. Crystallogr.*, 1969, **2**, 65–71.
7. Izumi, F., In *Rierveld Method*, ed. R. Young. Oxford University Press, Oxford, 1993 [chapter 13].
8. Hakki, B. W. and Coleman, P. D., A dielectric resonator method of measuring inductive in the millimeter range. *IRE Trans. Microwave Theory Tech.*, 1960, **MTT-8**, 402–410.
9. Penn, S. J., Alford, N. McN., Templeton, A., Wang, X., Xu, M., Reece, M. *et al.*, Effect of porosity and grain size on the microwave dielectric properties of sintered alumina. *J. Am. Ceram. Soc.*, 1997, **80**, 1885–1888.